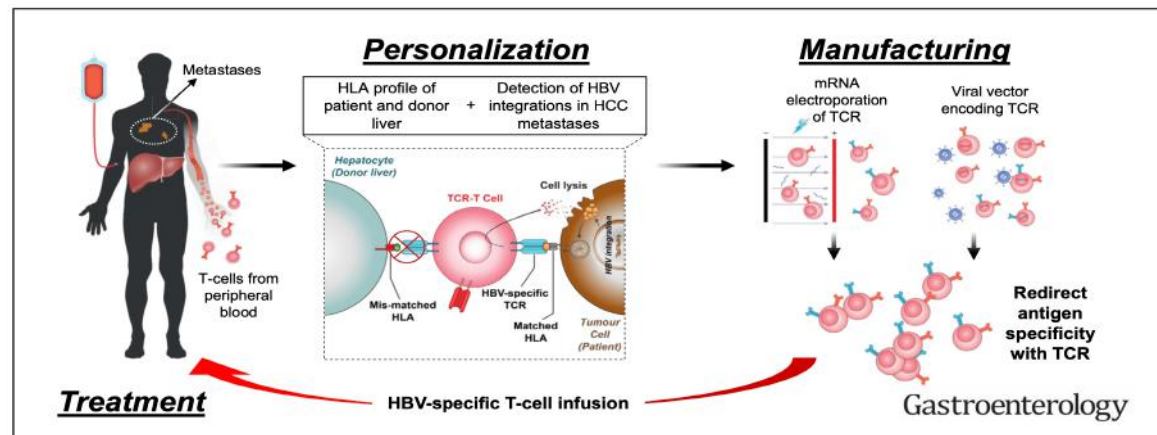




Use of Expression Profiles of HBV-DNA Integrated Into Genomes of Hepatocellular Carcinoma Cells to Select T Cells for Immunotherapy

Anthony Tanoto Tan,^{1,*} Ninghan Yang,^{2,*} Thinesh Lee Krishnamoorthy,^{3,*} Vincent Oei,¹ Alicia Chua,⁴ Xinyuan Zhao,⁴ Hui Si Tan,⁴ Adeline Chia,¹ Nina Le Bert,¹ Diana Low,⁵ Hiang Keat Tan,³ Rajneesh Kumar,³ Farah Gillan Irani,⁶ Zi Zong Ho,⁴ Qi Zhang,⁷ Ernesto Guccione,⁵ Lu-En Wai,^{4,8} Sarene Koh,^{4,8} William Hwang,⁹ Wan Cheng Chow,³ and Antonio Bertoletti^{1,8}

¹Emerging Infectious Diseases, Duke-NUS Medical School, Singapore; ²Genome Institute of Singapore, Agency for Science and Technology (A*STAR), Singapore; ³Department of Gastroenterology and Hepatology, Singapore General Hospital, Singapore; ⁴Lion TCR Pte Ltd, Singapore; ⁵Institute of Molecular and Cell Biology, Agency for Science and Technology (A*STAR), Singapore; ⁶Department of Vascular and Interventional Radiology, Singapore General Hospital, Singapore; ⁷Department of Biotherapy, The Third Affiliated Hospital of Sun Yat-Sen University, Guangdong, China; ⁸Singapore Immunology Network, Agency for Science and Technology (A*STAR), Singapore; ⁹Department of Haematology, Singapore General Hospital, Singapore



© 2019 by the AGA Institute. Published by Elsevier Inc. This is an open access article under the CC BY-NC-ND license (<http://creativecommons.org/licenses/by-nc-nd/4.0/>).

0016-5085
<https://doi.org/10.1053/j.gastro.2019.01.251>



Abstract

BACKGROUND & AIMS: Hepatocellular carcinoma (HCC) is often associated with hepatitis B virus (HBV) infection. Cells of most HBV-related HCCs contain HBV-DNA fragments that do not encode entire HBV antigens. We investigated whether these integrated HBV-DNA fragments encode epitopes that are recognized by T cells and whether their presence in HCCs can be used to select HBV-specific T-cell receptors (TCRs) for immunotherapy.

METHODS: HCC cells negative for HBV antigens, based on immunohistochemistry, were analyzed for the presence of HBV messenger RNAs (mRNAs) by real-time polymerase chain reaction, sequencing, and Nanostring approaches. We tested the ability of HBV mRNA-positive HCC cells to generate epitopes that are recognized by T cells using HBV-specific T cells and TCR-like antibodies. We then analyzed HBV gene expression profiles of primary HCCs and metastases from 2 patients with HCC recurrence after liver transplantation. Using the HBV-transcript profiles, we selected, from a library of TCRs previously characterized from patients with self-limited HBV infection, the TCR specific for the HBV epitope encoded by the detected HBV mRNA. Autologous T cells were engineered to express the selected TCRs, through electroporation of mRNA into cells, and these TCR T cells were adoptively transferred to the patients in increasing numbers (1×10^4 – 10×10^6 TCR+ T cells/kg) weekly for 112 days or 1 year. We monitored patients' liver function, serum levels of cytokines, and standard blood parameters. Antitumor efficacy was assessed based on serum levels of alpha fetoprotein and computed tomography of metastases.

RESULTS: HCC cells that did not express whole HBV antigens contained short HBV mRNAs, which encode epitopes that are recognized by and activate HBV-specific T cells. Autologous T cells engineered to express TCRs specific for epitopes expressed from HBV-DNA in patients' metastases were given to 2 patients without notable adverse events. The cells did not affect liver function over a 1-year period. In 1 patient, 5 of 6 pulmonary metastases decreased in volume during the 1-year period of T-cell administration.

CONCLUSIONS: HCC cells contain short segments of integrated HBV-DNA that encodes epitopes that are recognized by and activate T cells. HBV transcriptomes of these cells could be used to engineer T cells for personalized immunotherapy. This approach might be used to treat a wider population of patients with HBV-associated HCC.



HBV mRNA Fragments Are Present in HBV-HCC Cells With Undetectable HBV Antigens

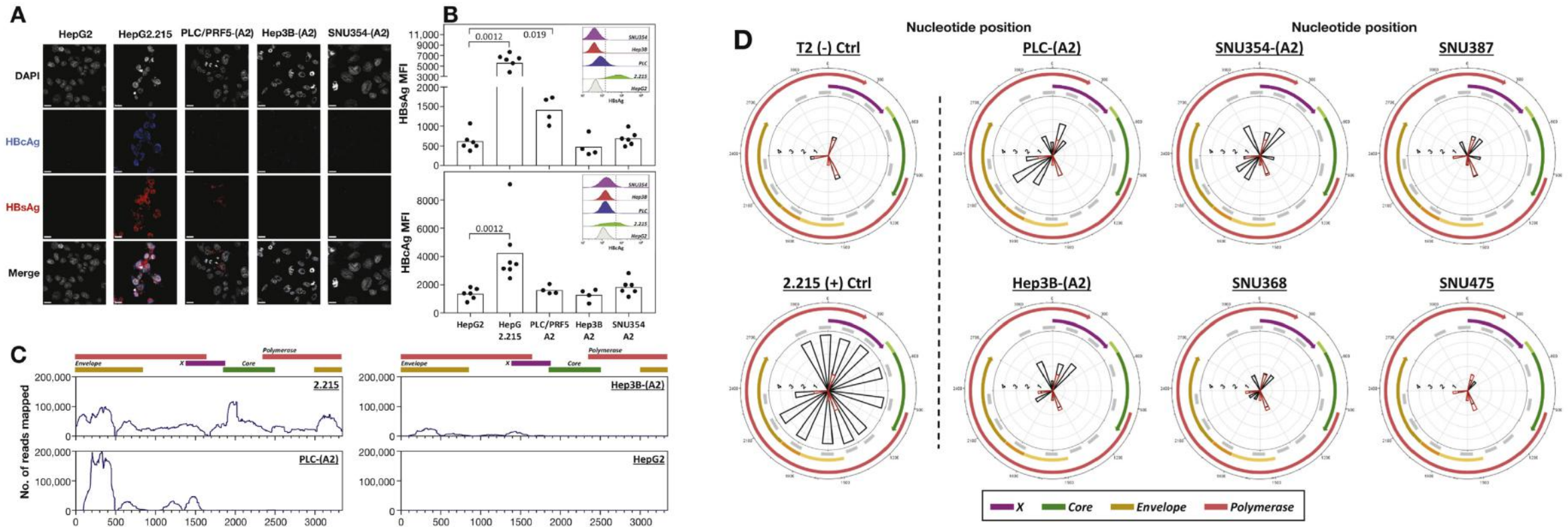


Figure 1. HBV-HCC lines negative for HBV antigens can contain fragments of HBV mRNA. (A) Immunofluorescence staining of HBV-HCC lines with HBsAg- (red), HBcAg-specific antibody (blue), and 4',6-diamidino-2-phenylindole (DAPI) (white). The scale bars are 15 μ m in length and the images are representative of 2 independent experiments. (B) Quantification of HBsAg and HBcAg expression in HBV-HCC lines by flow cytometry. Bars show the average geometric mean fluorescence intensities (MFI) and each circle denotes a single experiment. A representative experiment is shown in the histogram insert. Significant differences with $P < .05$ are indicated. (C) HBV-transcript profile of HBV-HCC lines obtained from Illumina high-throughput targeted sequencing using probes spanning across the entire HBV genome. Expression levels are shown as the number of reads mapped per nucleotide. (D) HBV-transcript profile of HBV-HCC lines (black) obtained using Nanostring probes covering the HBV genome. Radar plot shows the normalized counts of each HBV-specific probe expressed on a Log_{10} scale. The profile from HepG2 is overlaid in each radar plot (red). The open reading frames of HBV and relative positions of each Nanostring probe are annotated in a similar fashion to [Supplementary Figure 1](#).



Translation of HBV mRNA Fragments Generates Functional T-cell Epitopes

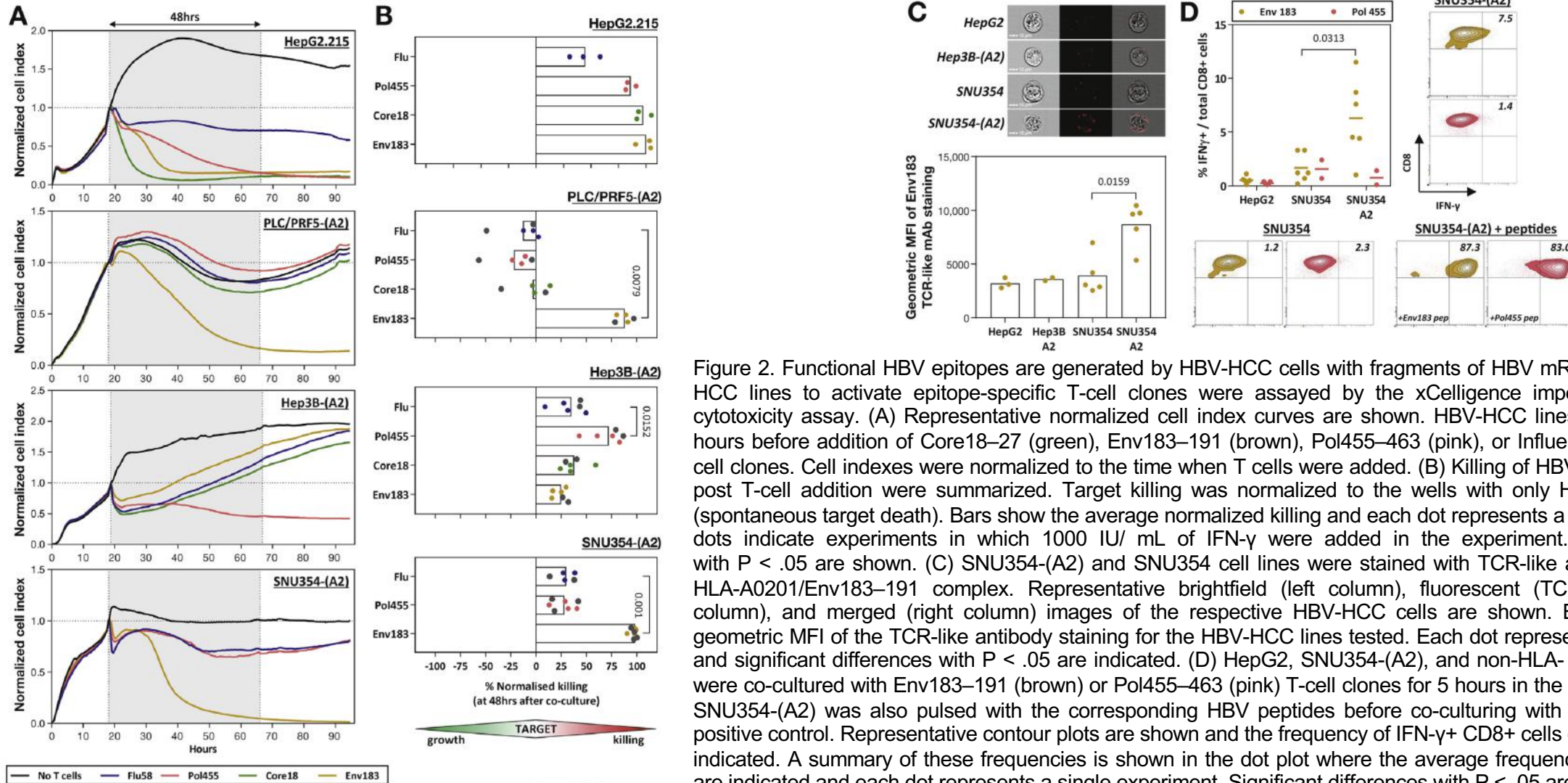


Figure 2. Functional HBV epitopes are generated by HBV-HCC cells with fragments of HBV mRNA. The ability of HBV-HCC lines to activate epitope-specific T-cell clones were assayed by the xCelligence impedance-based real-time cytotoxicity assay. (A) Representative normalized cell index curves are shown. HBV-HCC lines were cultured for ~18 hours before addition of Core18–27 (green), Env183–191 (brown), Pol455–463 (pink), or Influenza M1 58–66 (blue) T-cell clones. Cell indexes were normalized to the time when T cells were added. (B) Killing of HBV-HCC lines at 48 hours post T-cell addition were summarized. Target killing was normalized to the wells with only HBV-HCC lines cultured (spontaneous target death). Bars show the average normalized killing and each dot represents a single experiment. Gray dots indicate experiments in which 1000 IU/ mL of IFN- γ were added in the experiment. Significant differences with P < .05 are shown. (C) SNU354-(A2) and SNU354 cell lines were stained with TCR-like antibody specific for the HLA-A0201/Env183–191 complex. Representative brightfield (left column), fluorescent (TCR-like antibody; center column), and merged (right column) images of the respective HBV-HCC cells are shown. Bars show the average geometric MFI of the TCR-like antibody staining for the HBV-HCC lines tested. Each dot represents a single experiment and significant differences with P < .05 are indicated. (D) HepG2, SNU354-(A2), and non-HLA- A2 expressing SNU354 were co-cultured with Env183–191 (brown) or Pol455–463 (pink) T-cell clones for 5 hours in the presence of brefeldin-A. SNU354-(A2) was also pulsed with the corresponding HBV peptides before co-culturing with the T-cell clones as a positive control. Representative contour plots are shown and the frequency of IFN- γ + CD8+ cells of total CD8+ T cells are indicated. A summary of these frequencies is shown in the dot plot where the average frequency of IFN- γ + CD8+ cells are indicated and each dot represents a single experiment. Significant differences with P < .05 are indicated.



HBV-HCC Tissues Contain Short HBV mRNA Fragments Without HBsAg or HBcAg Expression

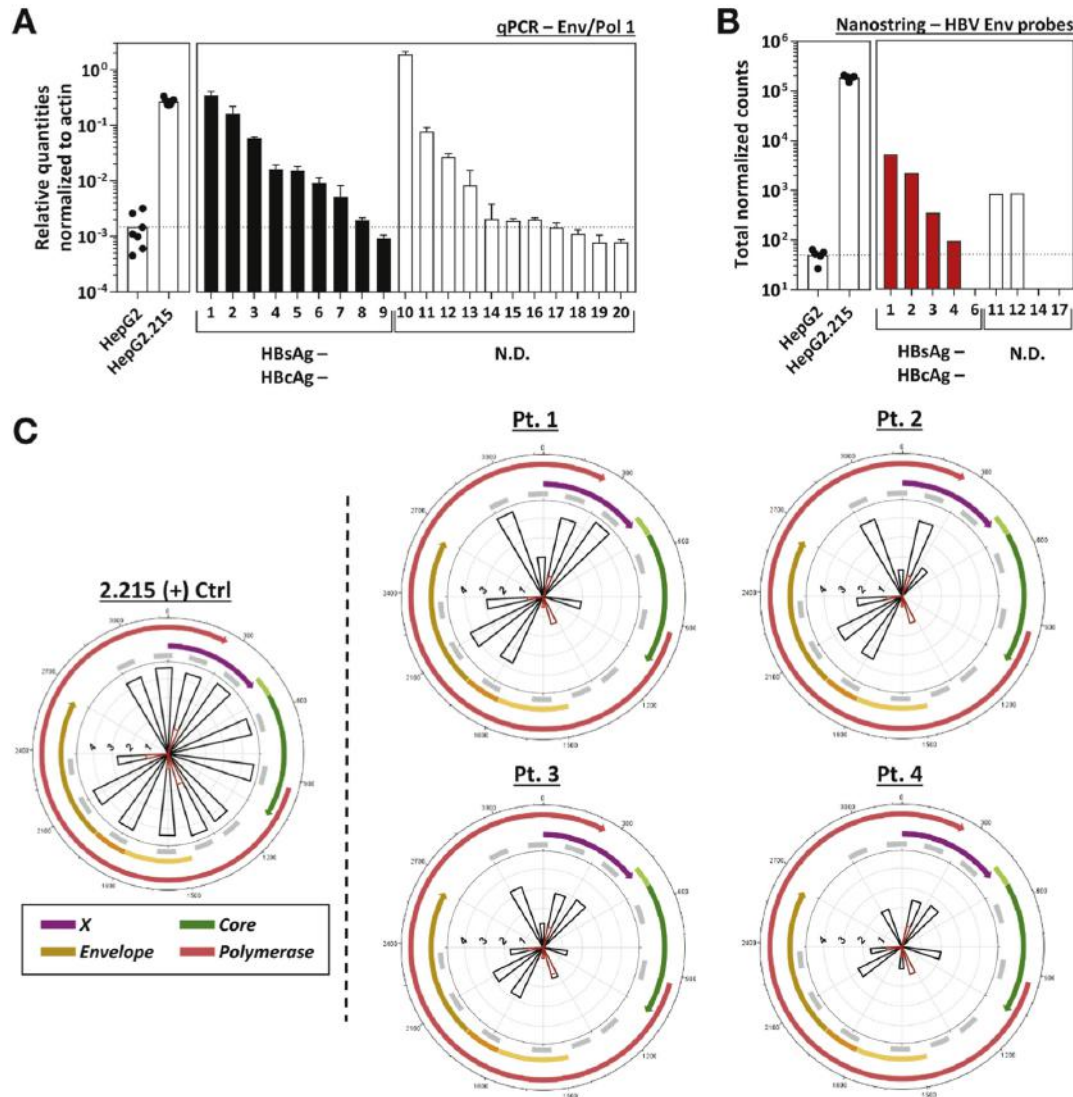


Figure 3. HBV mRNA fragments were found in tumor tissues of patients with HBV-related HCC. HBV envelope-specific mRNA transcripts were quantified in tumor tissues of patients with HBV-related HCC using, (A) qPCR primer pair Env/Pol 1 (n = 20) and (B) HBV-specific Nanostring probes (n = 9). Each analyzed patient is numbered and *solid bars* indicate HCC tissue samples that are HBsAg and HBcAg negative by immunohistochemistry. qPCR data were normalized to actin housekeeping controls. Normalized counts of HBV envelope-specific Nanostring probes (probes 1, 2, 3, and 12) were summed and shown in (B). HepG2 and HepG2.215 cells were also analyzed as controls and each dot represents a single experiment. (C) HBV-transcript profile of HCC tissues (*black*) obtained using Nanostring probes covering the HBV genome. Radar plots were annotated similar to Figure 1.



Profiling of HBV mRNA in Tumor Cells Guides Personalized T-cell Immunotherapy of HBV-HCC

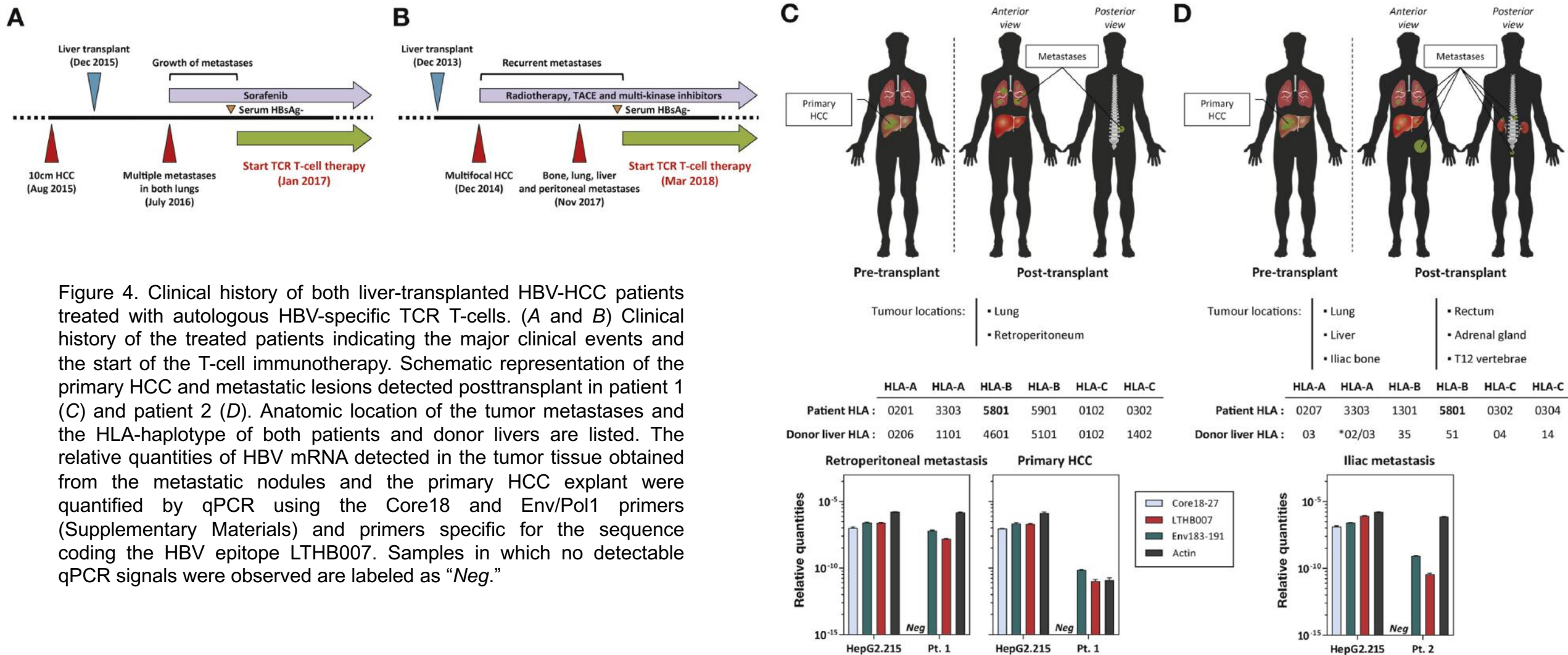


Figure 4. Clinical history of both liver-transplanted HBV-HCC patients treated with autologous HBV-specific TCR T-cells. (A and B) Clinical history of the treated patients indicating the major clinical events and the start of the T-cell immunotherapy. Schematic representation of the primary HCC and metastatic lesions detected posttransplant in patient 1 (C) and patient 2 (D). Anatomic location of the tumor metastases and the HLA-haplotype of both patients and donor livers are listed. The relative quantities of HBV mRNA detected in the tumor tissue obtained from the metastatic nodules and the primary HCC explant were quantified by qPCR using the Core18 and Env/Pol1 primers (Supplementary Materials) and primers specific for the sequence coding the HBV epitope LTHB007. Samples in which no detectable qPCR signals were observed are labeled as “Neg.”



Safety of the Autologous HBV-specific TCR T-cell Immunotherapy

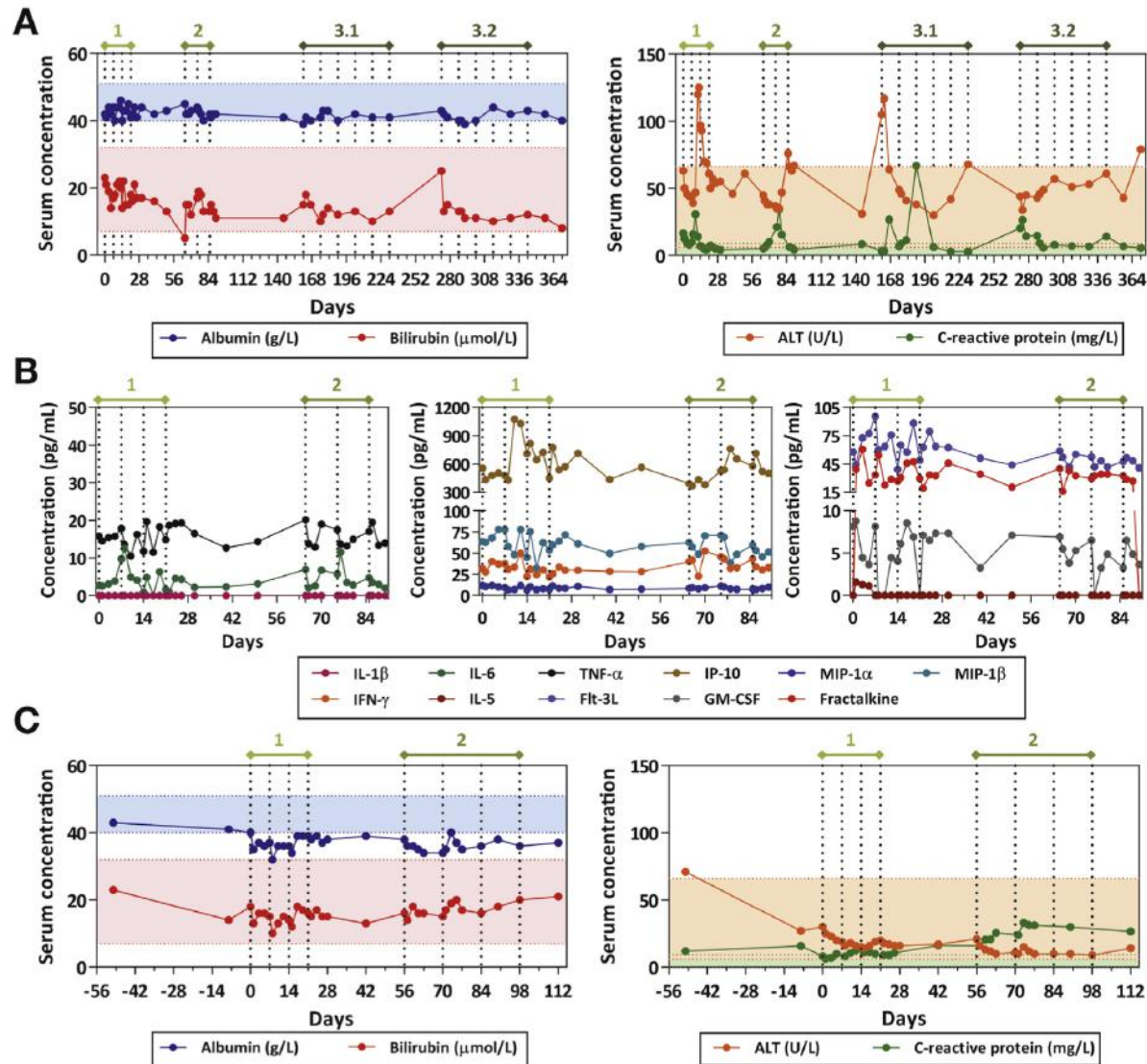


Figure 5. No therapy-related adverse events were observed in both patients treated with HBV-specific TCR T cells. Serum concentrations of albumin (*blue*), bilirubin (*red*), alanine aminotransferase (*orange*), and C-reactive protein (*green*) during the course of the T-cell immunotherapy in patient 1 (A) and patient 2 (C). Day 0 refers to the day of the first infusion. The colored areas represent the reference ranges for each parameter. Vertical dotted lines denote each TCR T-cell infusion and the different phases of the treatment are indicated. (B) Serum concentrations of cytokines, chemokines, and other soluble factors previously associated with severe cytokine release syndrome were analyzed in patient 1. The levels of these analytes were quantified during phases 1 and 2 of the treatment.



Efficacy of the Autologous HBV-specific TCR T-cell Immunotherapy

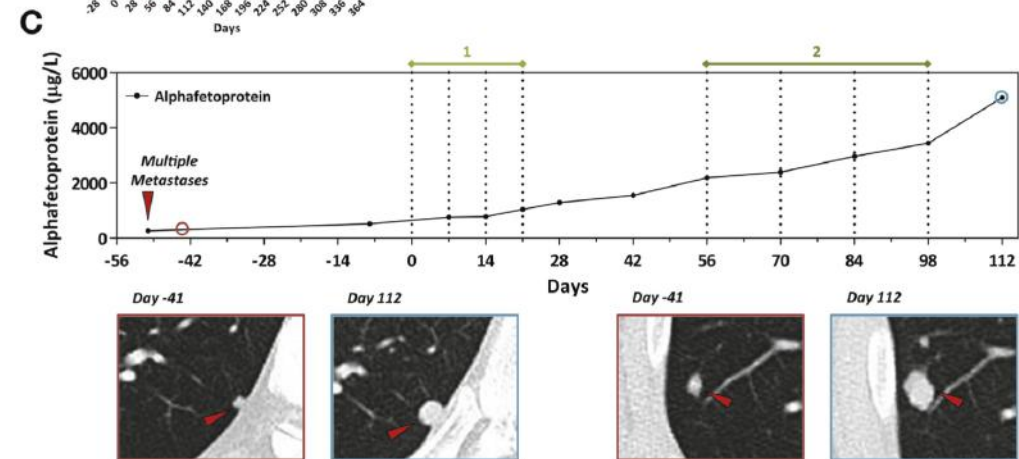
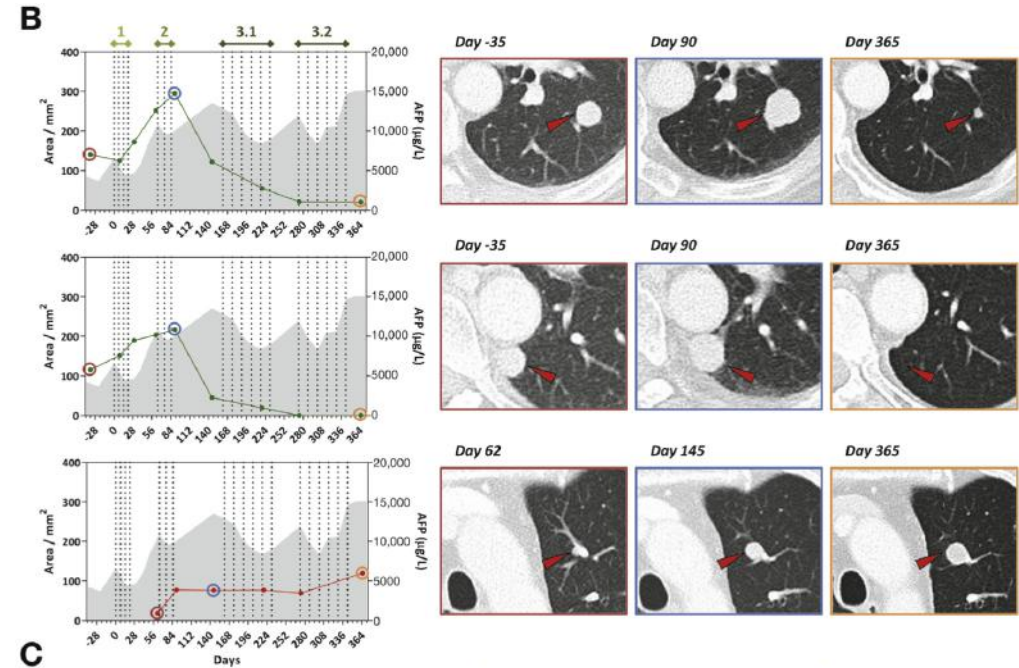
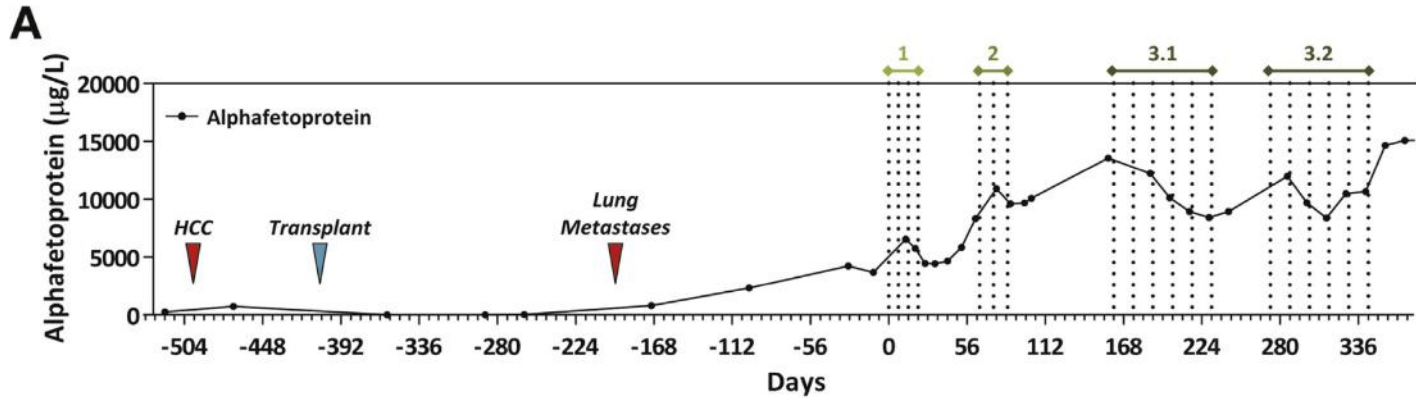


Figure 6. Monitoring of treatment response in both TCR T-cell-treated patients. Serum concentrations of AFP in patient 1 (A) and patient 2 (C) from before treatment until the end of the indicated treatment phases are shown. Vertical dotted lines denote each TCR T-cell infusion and the different phases of the treatment are indicated. (B) The largest cross-sectional area of all tumor nodules detected in the lungs of patient 1 (Supplementary Figure 8) were measured at specific intervals during the therapy and 3 representative nodules are shown. Gray-shaded areas represent the serum AFP concentrations. CT images of the corresponding tumor nodules at 3 indicated time points (*red*, *blue*, and *orange*) are shown and the lesions are indicated by the red arrow. (C) CT images of 2 representative tumor nodules in the lungs of patient 2 at the indicated time points (*red* and *cyan*) are shown and the lesions are indicated by the red arrow.